

Seven-Coordinate Dicarbonyl(triphenylphosphine)bis(*N,N*-dialkyldithio- carbamato)tungsten(II) Complexes. Molecular Structure and Dynamic Properties

Joseph L. Templeton* and Bennett C. Ward¹

Contribution from the W. R. Kenan, Jr. Laboratory, Department of Chemistry, University of North Carolina, Chapel Hill, North Carolina 27514. Received October 2, 1980

Abstract: The syntheses of a series of compounds of the type $W(CO)_2L(S_2CNR_2)_2$ are reported for $L =$ phosphine or phosphite. The crystal and molecular structure of one of these complexes, dicarbonyl(triphenylphosphine)bis(*N,N*-diethyldithiocarbamato)tungsten(II), has been determined by a single-crystal X-ray diffraction study. Dynamic ^{13}C NMR studies of $W(CO)_2L(S_2CNEt_2)_2$ ($L = PPh_3, PEt_3, P(OEt)_3$) revealed an intramolecular rearrangement process which averaged the two distinct carbon monoxide resonances observed in the low-temperature limit for each of the three complexes investigated. Crystals of $W(CO)_2(PPh_3)(S_2CNEt_2)_2$ were found to be triclinic of space group $P\bar{1}$ with unit cell dimensions of $a = 18.812$ (4) Å, $b = 20.133$ (6) Å, $c = 11.149$ (4) Å, $\alpha = 97.7$ (2)°, $\beta = 101.09$ (2)°, and $\gamma = 114.35$ (2)°. The observed density of 1.54 (1) g cm⁻³ is in agreement with a calculated value of 1.531 g cm⁻³ for $Z = 4$ with two toluene solvate molecules in the unit cell. The structure was refined to $R = 0.030$ and $R_w = 0.048$ by using 4475 reflections with $I > 3\sigma(I)$. The tungsten ion is seven-coordinate with an inner coordination sphere which can be conveniently described as conforming to a tetragonal base-trigonal base geometry. The structure and dynamic properties of $W(CO)_2L(S_2CNR_2)_2$ complexes are discussed with reference to previous studies characterizing related $W(CO)_3(S_2CNR_2)_2$ complexes. The prominent role of the d^4 configuration of the tungsten(II) ion present in $W(CO)_3(S_2CNR_2)_2$ complexes in labilizing one of the three π -acceptor carbonyl ligands to form dicarbonyl derivatives is discussed.

The chemistry of seven-coordinate compounds has expanded substantially during recent years.² Nonetheless chemical information relating to higher coordination numbers remains sparse compared to the extensive data base which has been compiled for lower coordination numbers, with six-coordinate compounds being particularly thoroughly investigated. The chemistry of molybdenum and tungsten d^4 complexes with π -acceptor ligands is dominated by seven-coordination in accord with expectations based on the effective atomic number rule.³ Two salient features which characterize the majority of seven-coordinate complexes studied to date include substantial deviations from any idealized geometry in the solid state⁴ and facile intramolecular rearrangements in solution.⁵ In several cases a detailed analysis of polytopal isomerization has been completed for seven-coordinate complexes and mechanistic information has been presented on the basis of variable-temperature NMR studies.⁶ Several examples of ste-

reochemically rigid seven-coordinate complexes have also been reported in the literature,⁷ but such behavior is still the exception rather than the rule.

Structural data for a large number of seven-coordinate complexes has become available during the past decade.⁸ Three idealized geometries (pentagonal bipyramid, D_{5h} , 1:5:1; capped octahedron, C_{3v} , 1:3:3; capped trigonal prism, C_{2v} , 1:4:2) are commonly employed as a point of departure for describing the ligand distribution in seven-coordinate compounds.⁹ Classification of an experimentally observed structure is particularly difficult for complexes with inequivalent and/or chelating ligands. Quantitative methods for assessing the deviation of observed structures from idealized polyhedra have been presented which provide the most rational method of accurately describing the inner coordination sphere of metal monomers.¹⁰ In an effort to match observed seven-coordinate geometries with an idealized model, we were led to consider the tetragonal base-trigonal base 4:3 description for $W(CO)_3(S_2CNR_2)_2$.¹¹ The simplicity of this model is attractive for purposes of visualization of the three-dimensional arrangement of ligating atoms, and hence the 4:3 provides a convenient basis for analyzing physical motions of the atoms which could be responsible for polytopal isomerization. The virtues of a simple classification scheme for seven-coordinate structures are apparent in the description of the $W(CO)_2(PPh_3)(S_2CNEt_2)_2$

(1) Eastman Kodak Fellow, 1979-1980.

(2) (a) Batschelet, W. H.; Archer, R. D.; Whitcomb, D. R. *Inorg. Chem.* **1979**, *18*, 48. (b) Bond, A. M.; Bixler, J. W.; Mocellin, E.; Datta, S.; James, E. J.; Wreford, S. S. *Ibid.* **1980**, *19*, 1760. (c) Domaille, P. J.; Foxman, B. M.; McNeese, T. J.; Wreford, S. S. *J. Am. Chem. Soc.* **1980**, *102*, 4114. (d) Peterson, E. J.; Von Dreelle, R. B.; Brown, T. M. *Inorg. Chem.* **1978**, *17*, 1410. (e) Bhat, A. N.; Fay, R. C.; Lewis, D. F.; Lindmark, A. F.; Strauss, S. H. *Ibid.* **1974**, *13*, 886. (f) Mattson, B. M.; Pignolet, L. H. *Ibid.* **1977**, *16*, 488. (g) Drew, M. G. B.; Wilkins, J. D. *J. Chem. Soc., Dalton Trans.* **1977**, 194. (h) Datta, S.; McNeese, T. J.; Wreford, S. S. *Inorg. Chem.* **1977**, *16*, 2661. (3) (a) Colton, R. *Coord. Chem. Rev.* **1971**, *6*, 269. (b) Ganorkar, M. C.; Stiddard, M. H. B. *J. Chem. Soc.* **1965**, 3494. (c) Bowden, J. A.; Colton, R. *Aust. J. Chem.* **1968**, *21*, 2657. (d) Lam, C. T.; Novotny, M.; Lewis, D. L.; Lippard, S. J. *Inorg. Chem.* **1978**, *17*, 2127. (e) Dreyer, E. B.; Lam, C. T.; Lippard, S. J. *Ibid.* **1979**, *18*, 1904. (f) Drew, M. G. B.; Wilkins, J. D. *J. Chem. Soc., Dalton Trans.* **1977**, 557. (g) Anker, M. W.; Colton, R.; Tomkins, I. B. *Rev. Pure Appl. Chem.* **1968**, *18*, 23. (4) (a) Datta, S.; Wreford, S. S. *Inorg. Chem.* **1977**, *16*, 1134. (b) Dewan, J. C.; Hendrick, K.; Kepert, D. L.; Trigwell, K. R.; White, A. H.; Wild, S. B. *J. Chem. Soc., Dalton Trans.* **1975**, 546. (c) Drew, M. G. B.; Walters, A. P.; Tomkins, I. B. *Ibid.* **1977**, 974. (d) Steffen, W. L.; Chun, H. K.; Fay, R. C. *Inorg. Chem.* **1978**, *17*, 3498. (5) (a) Muetterties, E. L. *Acc. Chem. Res.* **1970**, *3*, 266. (b) Pinnavia, T. J.; Fay, R. C. *Inorg. Chem.* **1968**, *7*, 502. (c) Wheeler, S. H.; Mattson, B. M.; Miessler, G. L.; Pignolet, L. H. *Ibid.* **1978**, *17*, 340. (d) Hoffmann, R.; Beier, B. F.; Muetterties, E. L.; Rossi, A. R. *Ibid.* **1977**, *16*, 511. (e) Chisholm, M. H.; Cotton, F. A.; Extine, M. W. *Ibid.* **1978**, *17*, 2000.

(6) (a) Albright, J. O.; Datta, S.; Dezube, B.; Kouba, J. K.; Marynick, D. S.; Wreford, S. S.; Foxman, B. M. *J. Am. Chem. Soc.* **1979**, *101*, 611. (b) Wreford, S. S.; Kouba, J. K.; Kirner, J. F.; Muetterties, E. L.; Tavanaiepour, I.; Day, V. W. *Ibid.* **1980**, *102*, 1558. (c) Domaille, P. J.; Wreford, S. S. *Inorg. Chem.* **1980**, *19*, 2188. (d) Byrne, J. W.; Krees, J. R. M.; Osborn, J. A.; Ricard, L.; Weiss, R. E. *J. Chem. Soc., Chem. Commun.* **1977**, 662. (e) Brown, L. D.; Datta, S.; Kouba, J. K.; Smith, L. K.; Wreford, S. S. *Inorg. Chem.* **1978**, *17*, 729.

(7) (a) Hawthorne, S. L.; Fay, R. C. *J. Am. Chem. Soc.* **1979**, *101*, 5268. (b) Davis, R.; Hill, M. N. S.; Holloway, C. E.; Johnson, B. F. G.; Al-Obaidi, K. H. *J. Chem. Soc. A* **1971**, 994. (c) Miessler, G. L.; Pignolet, L. H. *Inorg. Chem.* **1979**, *18*, 210.

(8) (a) Drew, M. G. B. *Prog. Inorg. Chem.* **1977**, *23*, 67. (b) Kepert, D. L. *Prog. Inorg. Chem.* **1979**, *25*, 41.

(9) Muetterties, E. L.; Wright, C. M. *Q. Rev., Chem. Soc.* **1967**, *21*, 109. (10) Muetterties, E. L.; Guggenberger, L. J. *J. Am. Chem. Soc.* **1974**, *96*, 1748.

(11) Templeton, J. L.; Ward, B. C. *Inorg. Chem.* **1980**, *19*, 1753.

geometry contained herein where comparison with the parent tricarbonyl complex is greatly facilitated by employing normalized bond lengths compatible with a 4:3 geometry. Our rationale for systematically probing seven-coordinate chemistry, defined to encompass structures, dynamic solution behavior, and reactivity patterns, is based on several salient features. Those facets most important for purposes of placing the content of this article in perspective are fourfold: (i) explore ligand substitution reactions of labile seven-coordinate compounds; (ii) seek cause and effect relationships for seven-coordinate geometries by examining structural details of related complexes for retention and/or alteration of coordination sphere parameters; (iii) assess the role of stereochemical nonrigidity in the solution behavior of diverse complexes; (iv) extend the data base for properties normally associated with d^4 metal ions bound to seven ligating atoms.

The work described herein addresses the above goals for complexes of the type $W(CO)_3(S_2CNR_2)_2$ and $W(CO)_2L(S_2CNR_2)_2$. Syntheses of $W(CO)_2L(S_2CNR_2)_2$ by substitution of the parent tricarbonyl are reported for a variety of phosphorus donor ligands. An X-ray structural determination of $W(CO)_2(PPh_3)(S_2CNEt_2)_2$ is reported and compared to that of the tricarbonyl complex $W(CO)_3(S_2CNMe_2)_2$. Dynamic exchange of the two carbonyl ligands has been observed for $W(CO)_2L(S_2CNR_2)_2$ complexes, and the implications of this rearrangement for understanding the two independent fluxional processes exhibited by $W(CO)_3(S_2CNR_2)_2$ are examined. The observed chemistry of $W(CO)_2L(S_2CNR_2)_2$ is compatible with expectations on the basis of the effective atomic number rule for a d^4 metal center where seven two-electron donors are required to satisfy the metal valence shell. This feature underscores the unique ligand properties which can profitably be expected to characterize related six-coordinate molybdenum(II) and tungsten(II) complexes¹² and promotes further studies of these complexes which invariably contain π -donor ligands.

Experimental Section

Materials and Procedure. All manipulations were performed either in a Vacuum Atmospheres drybox or by standard Schlenk techniques under an atmosphere of prepurified argon or nitrogen. Tetrahydrofuran was distilled from sodium benzophenone ketyl prior to use; all other solvents were dried over molecular sieves (4A) and purged with nitrogen gas before use.

Infrared spectra were recorded on a Beckman 4250 spectrophotometer and were calibrated with polystyrene. Nuclear magnetic resonance spectra [¹H (100 MHz), ¹³C (25.2 MHz), ³¹P (40.5 MHz)] were recorded on a Varian XL-100 spectrometer operating in the FT mode and were referenced to (Me₃Si)₂O, Me₄Si, and 85% H₃PO₄ for ¹H, ¹³C, and ³¹P, respectively. Tris(acetylacetonato)chromium(III) (10 mg) was added to ¹³C NMR samples as a shiftless paramagnetic relaxation agent.¹³ Tricarbonylbis(*N,N*-dialkyldithiocarbamate)tungsten(II) ($W(CO)_3(S_2CNR_2)_2$ with R = Me (**1a**) and R = Et (**1b**)) was prepared as described previously.¹¹

$W(CO)_2(PPh_3)(S_2CNMe_2)_2$ (**2a**). Solid **1a** (0.43 g, 0.85 mmol) and an excess of triphenylphosphine (0.40 g, 1.5 mmol) were placed in a Schlenk flask. Addition of toluene (20 mL) resulted in the formation of a red-orange solution. Slow gas evolution was observed as the solution was stirred for 3 h and a red-orange precipitate formed. The solid product was isolated by filtration and the volume of the orange filtrate was reduced in vacuo (5 mL) prior to the addition of cyclohexane (20 mL) which yielded additional product. The combined solids were rinsed with cyclohexane and dried under vacuum to yield **2a** (0.49 g, 78%): IR (Nujol mull) ν_{CO} 1909, 1821 cm⁻¹; ¹H NMR (CDCl₃) δ 3.04 (s, 12 H, CH₃), 7.31–7.36 (m, 15 H, C₆H₅); ¹³C{¹H} NMR (CDCl₃-CS₂) δ 38.7 (CH₃), 126.9–135.7 (C₆H₅), 233.2 (CO, -100 °C), 268.2 (CO, -100 °C). Compound **2a** is stable for several days in the solid state, but solutions exposed to air decompose in a few hours. Solutions of **2a** stored under

nitrogen showed no sign of decomposition over a period of weeks. A similar pattern of reactivity in air was observed for related tungsten(II)-carbonyl complexes described below.

$W(CO)_2(PPh_3)(S_2CNEt_2)_2$ (**2b**). Solid **1b** (0.42 g, 0.74 mmol) and an excess of triphenylphosphine (0.40 g, 1.5 mmol) were combined in a Schlenk flask, and toluene (20 mL) was added to form a red-orange solution with concomitant gas evolution. After 3 h the solution was filtered, the filtrate volume was reduced (5 mL), cyclohexane (20 mL) was added, and the flask was cooled in a freezer overnight to induce crystallization. The red-orange solid which precipitated was collected, washed with cyclohexane, and dried in vacuo to yield **2b** (0.51 g, 69%): IR (Nujol mull) ν_{CO} 1920, 1829 cm⁻¹; ¹H NMR (C₆D₆) δ 0.60 (t, 12 H, CH₃), 3.01 (q, 8 H, CH₂), 6.90–7.08 (m, 15 H, C₆H₅); ¹³C{¹H} NMR (CD₂Cl₂-CHClCH₂) δ 12.6 (CH₃, -40 °C), 44.3 (CH₂, -40 °C), 128.1–134.7 (C₆H₅, -40 °C), 232.9 (CO, -100 °C), 269.9 (CO, -100 °C); ³¹P NMR (CD₂Cl₂-CHClCH₂) δ -39.7.

$W(CO)_2(P(OEt)_3)(S_2CNR_2)_2$ (R = Me (**3a**) and R = Et (**3b**)). The procedures for preparation of **3a** and **3b** are identical; only the synthesis of **3a** is reported below. To a solution of **1a** (0.30 g, 0.59 mmol) in toluene (25 mL) was added an excess of triethylphosphite (0.12 g, 0.72 mmol) dissolved in toluene (10 mL). An orange-red solution formed and gas evolution was evident. After 14 h the solvent was removed in vacuo. The red oil which remained was treated with diethyl ether (2 mL) and hexane (20 mL). The resulting solution was cooled to -20 °C for 12 h to precipitate orange-red crystals of **3a** (0.28 g, 73%): IR (Nujol mull) ν_{CO} 1945, 1847 cm⁻¹; ¹H NMR (CS₂-C₆D₆) δ 1.12 (t, 9 H, CH₃ of P(OEt)₃), 2.98 (s, 12 H, CH₃ of S₂CNMe₂), 3.66 (m, 6 H, CH₂ of P(OEt)₃); ³¹P NMR (CS₂-C₆D₆) δ -151.9. **3b**: IR (CH₂Cl₂) ν_{CO} 1930, 1838 cm⁻¹; ¹H NMR (CS₂-C₆D₆) δ 1.01 (t, 12 H, CH₃ of S₂CNEt₂), 1.11 (t, 9 H, CH₃ of P(OEt)₃), 3.41 (q, 8 H, CH₂ of S₂CNEt₂), 3.80 (m, 6 H, CH₂ of P(OEt)₃); ¹³C{¹H} NMR (CD₂Cl₂-CHClCH₂, -25 °C) δ 12.5 (CH₃ of S₂CNEt₂), 16.2 (CH₃ of P(OEt)₃), 44.3 (CH₂ of S₂CNEt₂), 62.3 (CH₂ of P(OEt)₃), 229.2 (CO, -120 °C), 265.4 (CO, -120 °C).

$W(CO)_2(P(n-Bu)_3)(S_2CNR_2)_2$ (R = Me (**4a**) and R = Et (**4b**)). These complexes were prepared in a manner analogous to the synthesis of **3** described above. **4a**: IR (Nujol mull) ν_{CO} 1917, 1818 cm⁻¹; ¹H NMR (CS₂-C₆D₆) δ 0.82 (t, 9 H, CH₃ (8)), 1.28 (m, 6 H, CH₂ (8)), 1.80 (m, 6 H, CH₂ (α)), 2.86 (s, 12 H, CH₃ of S₂CNMe₂); ³¹P NMR (CS₂-C₆D₆) δ -5.04. **4b**: IR (Nujol mull) ν_{CO} 1915, 1825 cm⁻¹. ¹H NMR (CS₂-C₆D₆) δ 0.83 (t, 9 H, CH₃ (8)), 1.07 (t, 12 H, CH₃ of S₂CNEt₂), 1.28 (m, 6 H, CH₂ (β)), 1.80 (m, 6 H, CH₂ (α)), 3.47 (q, 8 H, CH₂ of S₂CNEt₂); ³¹P NMR (CS₂-C₆D₆) δ -5.11.

$W(CO)_2(Pt_3)(S_2CNEt_2)_2$ (**5b**). To a solution of **1b** (0.32 g, 0.157 mmol) in toluene (20 mL) was added an excess of triethylphosphine (0.10 g, 0.80 mmol) dissolved in toluene (10 mL). An orange solution formed and rapid gas evolution was observed. The solution was stirred for 2 h and then filtered, the solution volume was reduced (5 mL), cyclohexane was added (20 mL), and the solution was cooled to -20 °C overnight. The orange crystalline product was isolated by filtration, washed with cyclohexane, and dried in vacuo to yield **5b** (0.21 g, 70%): IR (toluene) ν_{CO} 1923, 1830 cm⁻¹. ¹H NMR (CDCl₃) δ 0.93 (m, 9 H, CH₃ (β)), 1.20 (t, 12 H, CH₃ of S₂CNEt₂), 1.91 (m, 6 H, CH₂ (α)), 3.66 (q, 8 H, CH₂ of S₂CNEt₂); ¹³C{¹H} NMR (C₇D₈-CHClCH₂, 0 °C) δ 8.3 (CH₃ (β), ²J_{C-P} = 3 Hz), 12.4 (CH₃ of S₂CNEt₂), 18.7 (CH₂ (α), ¹J_{C-P} = 29 Hz), 43.7 (CH₂ of S₂CNEt₂), 203.8 (S₂CNEt₂, ³J_{C-P} = 5 Hz, -110 °C), 233.4 (CO, -110 °C), 269.9 (CO, -110 °C); ³¹P NMR (C₇D₈) δ -12.7.

$W(^{13}CO)_2L(S_2CNR_2)_2$. Carbon-13-enriched complexes were prepared by reaction of the appropriate phosphorus ligand with $W(^{13}CO)_3(S_2CNR_2)_2$ ¹⁴ followed by isolation in the manner described above.

Collection and Reduction of X-ray Diffraction Data. A single crystal of **2b** suitable for data collection was grown by slow diffusion of cyclohexane into a saturated toluene solution. A dark orange-red hexagonal block of approximate dimensions 0.40 × 0.39 × 0.17 mm was mounted on a glass fiber, coated with epoxy cement, and transferred to an Enraf-Nonius CAD-4 automated diffractometer. Additional crystal data are presented in Table I. Program SEARCH was used to obtain 25 well-centered reflections.¹⁵ The angular settings for these reflections were then used by the program INDEX to calculate the unit cell dimensions for a triclinic cell. Program TRACER indicated that the cell was indeed triclinic. Accurate cell constants (Table I) and their estimated standard deviations were obtained by least-squares refinement of the 25 reflections.

Preliminary analysis of the diffractometer data revealed no systematic absences, indicating a triclinic space group (P1 or P1̄). The observed

(12) (a) Templeton, J. L.; Ward, B. C. *J. Am. Chem. Soc.* **1980**, *102*, 6568. (b) Ricard, L.; Weiss, R.; Newton, W. E.; Chen, G. J.-J.; McDonald, J. W. *Ibid.* **1978**, *100*, 1318. (c) Ward, B. C.; Templeton, J. L. *Ibid.* **1980**, *102*, 1532. (d) Chisholm, M. H.; Huffman, J. C.; Kelly, R. L. *Ibid.* **1979**, *101*, 7615. (e) Haymore, B. L.; Maatta, E. A.; Wentworth, R. A. D. *Ibid.* **1979**, *101*, 2063. (f) Johnson, B. F. G.; Al-Obaidi, K. H.; McCleverty, J. A. *J. Chem. Soc. A* **1969**, 1668.

(13) (a) Gansow, O. A.; Burke, A. R.; Vernon, W. O. *J. Am. Chem. Soc.* **1972**, *94*, 2550. (b) Cotton, F. A.; Hunter, D. L.; White, A. J. *Inorg. Chem.* **1975**, *14*, 703.

(14) Templeton, J. L. *Adv. Chem. Ser.* **1979**, No. 173, 263.

(15) All programs utilized during data collection were provided by Enraf-Nonius. All programs used for structure solution and refinement were part of the Structure Determination Package (SDP) provided by B. Frenz through Enraf-Nonius.

Table I. Crystal and Data Collection Parameters for $W(\text{CO})_2(\text{P}(\text{C}_6\text{H}_5)_3)(\text{S}_2\text{CN}(\text{CH}_2\text{CH}_3)_2)_2 \cdot 1/2 \text{C}_6\text{H}_5\text{CH}_3$

a. Crystal and Lattice Parameters	
$a = 18.812$ (4) Å	space group $P1$ (C_1 , No. 2)
$b = 20.133$ (6) Å	$Z = 4$
$c = 11.149$ (4) Å	$V = 3666$ (5) Å ³
$\alpha = 97.70$ (2)°	$\rho_{\text{obsd}}(\text{CCl}_4\text{-C}_6\text{H}_{12}) = 1.54$ (1) g cm ⁻³
$\beta = 101.09$ (2)°	$\rho_{\text{calcd}} = 1.531$ g cm ⁻³
$\gamma = 114.35$ (2)°	$\mu(\text{Mo K}\alpha) = 36.3$ cm ⁻¹
empirical formula: $\text{W}_2\text{S}_8\text{P}_2\text{O}_4\text{N}_4\text{C}_{67}\text{H}_{78}$	
b. Data Collection Parameters	
radiation	Mo K α ($\lambda = 0.71069$ Å)
monochromator	graphite crystal
takeoff angle	2.6°
reflections measd	$\pm h, \pm k, +l$
scan mode	$w = 4/3 \theta$
scan range	$2^\circ \leq 2\theta \leq 40^\circ$
scan width	$(A + B \tan \theta)^\circ$, $A = 0.80^\circ$, $B = 0.35^\circ$
scan rate	variable (1.5–10° min ⁻¹)
prescan rate	10° min ⁻¹
bkgd scan width	25% of peak width on each side

density of 1.54 (1) g cm⁻³ compares with $\rho_{\text{calcd}} = 1.531$ g cm⁻³ for $Z = 4$ with two molecules of **2b** and a toluene molecule in the asymmetric unit. A unique hemisphere of data ($\pm h, \pm k, +l$) was collected under the conditions reported in Table I. Reflection intensity and crystal orientation were monitored periodically throughout data collection by measuring a set of standard reflections. Intensity measurements did not vary below 90% of the original intensity for the standards monitored, and the crystal was reoriented when the scattering vector varied by more than 0.15°.

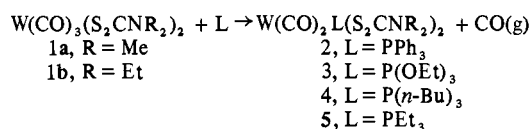
The raw intensity data were reduced and corrected for absorption ($\mu = 36.3$ cm⁻¹) by an empirical method based on ψ scans of nine reflections with $80^\circ \leq X \leq 90^\circ$. The data were also corrected for Lorentz-polarization effects. A total of 7121 independent reflections were processed of which 5199 had $I \geq 3\sigma(I)$ where $\sigma(I)$ is

$$\sigma(I) = [S^2(C + RB)^2 + (pI)^2]^{1/2}$$

with S the scan rate, C the total counts, R the ratio of the peak scan time to the total scan time (here equal to 2), B the total background count, and p the correction factor which was set at 0.04. Data with $I \geq 3\sigma(I)$ and with $3 \leq 2\theta \leq 38^\circ$ (4475) were used in the refinement of the structure due to time and space limitations of the PDP 11/34 computer memory.

Solution and Refinement of the Crystal Structure. The positions of the two independent tungsten atoms were located by means of a three-dimensional Patterson function. The tungsten positions were refined by full-matrix, least-squares techniques. The refinement was carried out on F with the function minimized being $\sum w(|F_o| - |F_c|)^2$, where the weights, w , were taken as $w = (2F_o/\sigma(F_o))^2$ and F_o and F_c are the observed and calculated structure amplitudes. The atomic scattering factors used in the calculations were taken from Cromer and Waber,^{16a} and the anomalous dispersion factors were taken from Cromer.^{16b} All remaining nonhydrogen atoms in the two independent molecules of **2b** were located in subsequent difference Fourier maps, with the phenyl carbons and alkyl carbons being refined isotropically while all other heavy atoms were refined anisotropically to give values of the unweighted and weighted residuals, $R = \sum(|F_o| - |F_c|)/\sum|F_o|$ and $R_w = [\sum w(|F_o| - |F_c|)^2 / \sum w|F_o|^2]^{1/2}$, of 0.053 and 0.082, respectively. At this stage a difference Fourier map revealed the atom positions of a single toluene molecule in the asymmetric unit. The carbon atoms of this solvent molecule did not refine well and exhibited large isotropic thermal parameters and unreasonable bond distances and angles. This may be due to the solvent fitting loosely in the cell combined with the overwhelming contribution of the other 80 heavy atoms to the model. Refinement of the solvent molecule parameters was not considered essential, and the refinement was terminated on the basis of convergence of the parameters of the two independent molecules of **2b**. The agreement between analogous bond distances and angles of the two independent molecules of **2b** is indicative of the accuracy of structure with regard to the metal complex. The positions of the toluene atoms were held constant in the final cycle of

Scheme I



least-squares refinement where 4475 observations and 461 variables provided a data to variable ratio of 9.7:1. The fact that no parameter shifted by more than 0.1 σ was taken as evidence of convergence. The final values of R and R_w were 0.030 and 0.048, respectively, and the ESD of an observation of unit weight was 1.67. The final difference Fourier map was featureless, with the highest peak corresponding to 0.38 e Å⁻³.

The atomic positional and thermal parameters are found in Tables II and III, respectively. Observed and calculated structure factors are available as supplementary material.

Results and Discussion

Syntheses. Seven-coordinate compounds of the type $\text{M}(\text{CO})_2(\text{PPh}_3)(\text{S}_2\text{CNR}_2)_2$ were first prepared by Colton and Rose for $\text{M} = \text{Mo}$ from the reaction of $\text{Mo}(\text{CO})_3(\text{PPh}_3)_2\text{Cl}_2$ with dithiocarbamate salts.¹⁷ In 1977 McDonald and co-workers succeeded in preparing the analogous tungsten derivative after an improved preparative route was developed to $\text{W}(\text{CO})_3(\text{PPh}_3)_2\text{Cl}_2$ which was used as a reagent in their synthetic scheme.¹⁸ The recent synthesis of $\text{W}(\text{CO})_3(\text{S}_2\text{CNR}_2)_2$ (**1**)¹⁴ provides a convenient vehicle for a generic preparative route to substituted $\text{W}(\text{CO})_2\text{L}(\text{S}_2\text{CNR}_2)_2$ derivatives where L is a neutral phosphorus donor ligand. The reaction of **1** with excess phosphine or phosphite nucleophiles proceeds at room temperature as indicated in Scheme I to form monosubstituted $\text{W}(\text{CO})_2\text{L}(\text{S}_2\text{CNR}_2)_2$ derivatives which can be isolated as crystalline solids varying from orange to red in color. Only compound **2** has been reported previously, and the method of synthesis in that case is limited to $\text{L} = \text{PPh}_3$.¹⁸

The facility with which substitution of a single carbon monoxide ligand in **1** occurs is not unexpected in view of the reversible dissociation of carbon monoxide to form a 16-electron dicarbonyl complex which has been reported for **1**¹⁴ and $\text{Mo}(\text{CO})_3(\text{S}_2\text{CNR}_2)_2$ ^{12a,19} (see eq 1). Note that loss of carbon monoxide



from $\text{M}(\text{CO})_2\text{L}(\text{S}_2\text{CNR}_2)_2$ to form $\text{M}(\text{CO})\text{L}(\text{S}_2\text{CNR}_2)_2$ has not been observed. Presumably this reactivity difference reflects the more limited metal d to carbonyl π^* bonding per carbonyl ligand present in the parent tricarbonyl complex.

Support for differences in metal-carbonyl bonding can be gleaned from crude force constant calculations which assume local C_{3v} and C_{2v} symmetry for the tricarbonyl and dicarbonyl compounds, respectively. Admittedly such an assumption is incorrect since the carbonyls do not occupy equivalent positions in the coordination sphere of the tungsten. Nonetheless the approximate carbon monoxide force constants derived from application of the Cotton-Kraihanzel analysis as formulated for $\text{ML}_{6-n}(\text{CO})_n$ ²⁰ at least serve as a qualitative guide to the strength of the coordinated C–O bond and are preferable to observed vibrational frequencies for purposes of comparison among the $\text{ML}_m(\text{CO})_n$ complexes listed in Table IV with $n = 2$ or 3. The decrease in k_{CO} evident in comparing $\text{M}(\text{CO})_3(\text{S}_2\text{CNR}_2)_2$ with either the six-coordinate $\text{M}(\text{CO})_2(\text{S}_2\text{CNR}_2)_2$ or the seven-coordinate $\text{M}(\text{CO})_2\text{L}(\text{S}_2\text{CNR}_2)_2$ complexes is large enough to qualitatively discriminate between the extent of metal to carbonyl back-bonding in these cases. The proximity of the carbonyl stretching frequencies observed for both six- and seven-coordinate dicarbonyl derivatives is directly reflected in the corresponding carbon monoxide force constants. The similar values of k_{CO} for these complexes suggest that the extent of π -electron density provided by the d⁴ metal ion to the two carbonyl ligands is nearly independent of (i) the coordination number (six

(17) Colton, R.; Rose, G. G. *Aust. J. Chem.* **1970**, *23*, 1111.(18) Chen, G. J.-J.; Yelton, R. O.; McDonald, J. W. *Inorg. Chim. Acta* **1977**, *22*, 249.(19) (a) Colton, R.; Scollary, G. R. *Aust. J. Chem.* **1968**, *21*, 1427. (b) Colton, R.; Scollary, G. R.; Tomkins, I. B. *Ibid.* **1968**, *21*, 15.(20) Cotton, F. A.; Kraihanzel, C. S. *J. Am. Chem. Soc.* **1962**, *84*, 4432.(16) (a) Cromer, D. T.; Waber, J. T. "International Tables for X-Ray Crystallography"; Ibers, J. A., Hamilton, W. C., Eds.; Kynoch Press: Birmingham, England, 1974; Vol. IV, Table 2.2A. (b) Cromer, D. T. *Ibid.*, Table 2.3.1.

Table II. Final Atomic Positional Parameters for 2b^a

atom	x	y	z	atom	x	y	z
W	0.24293 (3)	0.49040 (2)	0.04426 (5)	C3B	0.3439 (6)	0.5788 (6)	0.378 (1)
W'	0.18121 (3)	0.01601 (2)	0.41137 (5)	C4B	0.4682 (7)	0.7133 (6)	0.528 (1)
S4	0.2530 (2)	0.4458 (2)	0.8248 (3)	C5B	0.4001 (7)	0.6786 (7)	0.571 (1)
S3	0.3434 (2)	0.4366 (2)	0.0576 (3)	C6B	0.3329 (7)	0.6069 (6)	0.492 (1)
S2	0.1326 (2)	0.3574 (2)	0.0137 (3)	C1C	0.1752 (6)	0.4696 (6)	0.333 (1)
S1	0.1100 (2)	0.4731 (2)	0.9139 (3)	C2C	0.116 (7)	0.4402 (7)	0.502 (1)
S'4	0.9720 (2)	0.0558 (2)	0.6282 (3)	C3C	0.1788 (7)	0.4537 (6)	0.450 (1)
S'3	0.1421 (2)	0.8914 (2)	0.4741 (3)	C4C	0.0418 (7)	0.4402 (7)	0.429 (1)
S'2	0.1557 (2)	0.9545 (2)	0.1812 (3)	C5C	0.9612 (7)	0.5446 (7)	0.688 (1)
S'1	0.1346 (2)	0.0825 (2)	0.2662 (3)	C6C	0.1076 (7)	0.4716 (6)	0.259 (1)
P1	0.2633 (2)	0.4902 (2)	0.2716 (3)	C'5	0.1027 (9)	0.1864 (8)	0.560 (2)
P'1	0.3147 (2)	0.0150 (2)	0.4389 (3)	C'6	0.1436 (11)	0.2321 (10)	0.686 (2)
O2	0.3887 (5)	0.633 (5)	0.0233 (9)	C'7	0.0000 (8)	0.7642 (7)	0.526 (1)
O1	0.2356 (4)	0.6336 (4)	0.1688 (9)	C'8	-0.0049 (10)	0.2176 (9)	0.337 (2)
O'2	0.1713 (5)	0.0664 (5)	0.6809 (8)	C'9	0.0952 (8)	0.0922 (7)	-0.007 (1)
O'1	0.3098 (5)	0.1834 (4)	0.5302 (8)	C'10	0.1722 (10)	0.1592 (9)	0.989 (2)
N2	0.3689 (6)	0.4010 (5)	0.8360 (10)	C'11	0.1122 (8)	0.9742 (8)	0.913 (1)
N1	-0.0126 (5)	0.3361 (5)	0.8769 (10)	C'12	0.1996 (10)	-0.0048 (9)	0.912 (2)
N'2	0.9852 (6)	0.8226 (5)	0.4647 (11)	C'1A	0.3843 (6)	0.0668 (5)	0.594 (1)
N'1	0.1152 (6)	0.0295 (5)	0.0206 (9)	C'2A	0.5364 (7)	0.8807 (6)	0.390 (1)
C2	0.3344 (6)	0.5816 (6)	0.031 (1)	C'3A	0.4861 (8)	0.8378 (7)	0.267 (1)
C1	0.2351 (6)	0.5777 (6)	0.125 (1)	C'4A	0.4822 (8)	0.1512 (7)	0.840 (1)
C4	0.3285 (6)	0.4261 (6)	0.898 (1)	C'5A	0.4027 (7)	0.0958 (7)	0.821 (1)
C3	0.0659 (6)	0.3817 (6)	0.928 (1)	C'6A	0.3533 (6)	0.0548 (6)	0.698 (1)
C'2	0.1751 (6)	0.0480 (6)	0.582 (1)	C'1B	0.3729 (7)	0.0549 (6)	0.328 (1)
C'1	0.2640 (7)	0.1215 (6)	0.482 (1)	C'2B	0.4794 (9)	0.0665 (8)	0.225 (1)
C'4	0.0438 (7)	0.8783 (6)	0.440 (1)	C'3B	0.4610 (8)	0.1165 (8)	0.167 (1)
C'3	0.1319 (7)	0.0216 (6)	0.138 (1)	C'4B	0.4334 (8)	0.0342 (7)	0.312 (1)
C5	0.3616 (8)	0.4001 (7)	0.699 (1)	C'5B	0.3532 (7)	0.1024 (6)	0.266 (1)
C6	0.4153 (9)	0.4774 (8)	0.689 (2)	C'6B	0.3986 (8)	0.1347 (7)	0.179 (1)
C7	0.4334 (8)	0.3833 (7)	0.904 (1)	C'1C	0.3137 (6)	0.9231 (6)	0.421 (1)
C8	0.3945 (10)	0.2985 (10)	0.892 (2)	C'2C	0.2819 (7)	0.8762 (6)	0.300 (1)
C9	0.0695 (7)	0.6376 (6)	0.186 (1)	C'3C	0.2795 (7)	0.8040 (6)	0.287 (1)
C10	0.0818 (8)	0.6560 (7)	0.330 (1)	C'4C	0.3076 (7)	0.7807 (6)	0.389 (1)
C11	0.9510 (7)	0.2567 (7)	0.893 (1)	C'5C	0.3395 (7)	0.8290 (7)	0.508 (1)
C12	0.0804 (9)	0.7460 (8)	-0.008 (2)	C'6C	0.3435 (7)	0.9013 (6)	0.525 (1)
C1A	0.2354 (7)	0.3454 (6)	0.297 (1)	C1''	0.2485 (0)	0.6899 (0)	0.825 (0)
C2A	0.2607 (7)	0.2901 (7)	0.320 (1)	C2''	0.2937 (0)	0.7564 (0)	0.917 (0)
C3A	0.3424 (7)	0.3092 (7)	0.357 (1)	C3''	0.3235 (0)	0.8379 (0)	0.960 (0)
C4A	0.4026 (7)	0.3816 (7)	0.373 (1)	C4''	0.3063 (0)	0.8776 (0)	0.898 (0)
C5A	0.3775 (6)	0.4379 (6)	0.351 (1)	C5''	0.2441 (0)	0.8129 (0)	0.768 (0)
C6A	0.2956 (6)	0.4199 (5)	0.314 (1)	C6''	0.2101 (0)	0.7424 (0)	0.710 (0)
C1B	0.4135 (6)	0.6153 (6)	0.338 (1)	C7''	0.2044 (0)	0.6482 (0)	0.731 (0)
C2B	0.5238 (7)	0.3144 (6)	0.581 (1)				

^a Numbers in parentheses are the estimated standard deviations of the coordinates and refer to the last significant digit of the preceding number.

or seven) and (ii) the identity of the phosphorus donor ligand in the seven-coordinate monomers reported.

Substitution of a second carbon monoxide ligand in **1** to form $W(CO)(L)_2(S_2CNR_2)_2$ has not been observed with monodentate phosphine or phosphite ligands. The potentially bidentate bis-(diphenylphosphino)ethane (dppe) ligand initially reacts with **1** to form a monodentate dicarbonyl derivative before slowly losing a second carbonyl ligand and binding the second phosphorus atom to yield $W(CO)(dppe)(S_2CNR_2)_2$.²¹ The relative inertness of seven-coordinate d^4 dicarbonyl complexes is reminiscent of the substitution chemistry of six-coordinate d^6 tricarbonyl derivatives where *fac*- $M(CO)_3L_3$ complexes form readily but resist further carbonyl substitution.²² It seems probable that the electron configuration of the metal plays a key role in these reactivity patterns with two and three carbonyl π -acceptor ligands optimal for d^4 and d^6 ions, respectively. The ease with which $M(CO)_2L(S_2CNR_2)_2$ ($M = Mo$ or W) complexes form from tricarbonyl compounds and the difficulty of achieving formation of $M(CO)L_2(S_2CNR_2)_2$ by substitution of a carbonyl ligand support this generalization.

Molecular Structure of 2b. The molecular structure of **2b** is illustrated in Figure 1. The X-ray structure solution revealed two independent molecules of **2b** and a single toluene molecule

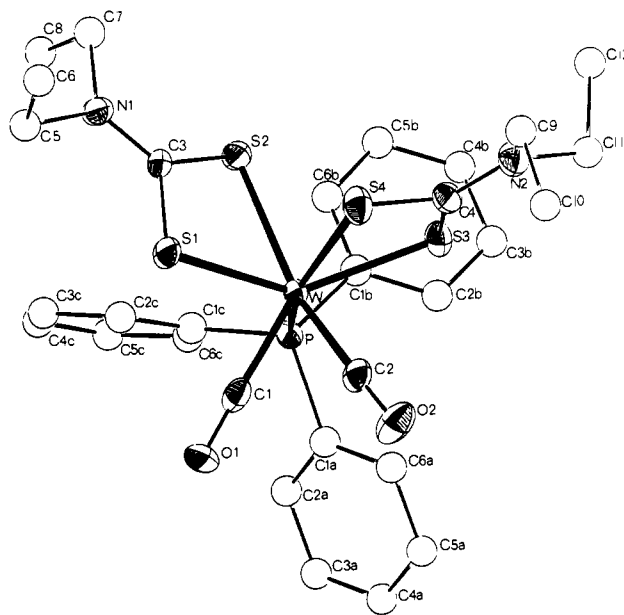


Figure 1. A view of one of the independent molecules of **2b** showing the atomic labeling scheme. Anisotropic thermal ellipsoids are drawn at the 25% probability level, and isotropic spheres are of arbitrary size.

(21) Ward, B. C.; Templeton, J. L., unpublished results.

(22) (a) Abel, E. W.; Bennett, M. A.; Wilkinson, G. *J. Chem. Soc.* **1959**, 2325. (b) Tate, D. P.; Knipple, W. R.; Augl, J. M. *Inorg. Chem.* **1962**, *1*, 433.

Table III

(a) Final Anisotropic Thermal Parameters for 2b

atom	U_{11}^a	U_{22}	U_{33}	U_{12}	U_{13}	U_{23}
W	0.0369 (2)	0.0401 (2)	0.0511 (3)	0.0176 (2)	0.0096 (2)	0.0094 (2)
S4	0.059 (2)	0.089 (2)	0.048 (2)	0.038 (1)	0.013 (2)	0.013 (2)
S3	0.057 (2)	0.076 (2)	0.054 (2)	0.043 (1)	0.014 (2)	0.014 (2)
S2	0.049 (2)	0.044 (2)	0.068 (2)	0.019 (1)	0.088 (2)	0.011 (2)
S1	0.041 (2)	0.051 (2)	0.072 (2)	0.019 (1)	0.005 (2)	0.018 (2)
P1	0.044 (2)	0.041 (2)	0.054 (2)	0.019 (1)	0.015 (2)	0.010 (2)
O2	0.055 (5)	0.081 (5)	0.108 (7)	0.010 (4)	0.020 (5)	0.042 (5)
O1	0.070 (4)	0.046 (4)	0.103 (7)	0.033 (3)	0.011 (5)	0.002 (4)
N2	0.079 (6)	0.089 (6)	0.055 (7)	0.049 (4)	0.010 (5)	0.010 (5)
N1	0.041 (5)	0.041 (5)	0.077 (7)	0.016 (4)	0.005 (5)	0.005 (5)
C2	0.043 (6)	0.064 (6)	0.063 (8)	0.028 (4)	0.001 (6)	0.017 (6)
C1	0.036 (6)	0.056 (6)	0.075 (9)	0.017 (5)	0.007 (6)	0.029 (6)
C4	0.059 (6)	0.072 (7)	0.058 (8)	0.035 (5)	0.022 (6)	0.001 (7)
C3	0.050 (6)	0.051 (6)	0.063 (8)	0.028 (4)	0.017 (6)	0.009 (6)
W'	0.0474 (3)	0.0380 (2)	0.0402 (3)	0.0177 (2)	0.0090 (2)	0.0114 (2)
S'4	0.052 (2)	0.063 (2)	0.076 (2)	0.025 (1)	0.014 (2)	0.030 (2)
S'3	0.051 (2)	0.054 (2)	0.080 (2)	0.026 (1)	0.022 (2)	0.031 (2)
S'2	0.069 (2)	0.046 (2)	0.044 (2)	0.025 (1)	0.003 (2)	0.005 (1)
S'1	0.075 (2)	0.047 (1)	0.048 (2)	0.030 (1)	0.007 (2)	0.015 (1)
P'1	0.044 (2)	0.044 (2)	0.038 (2)	0.014 (1)	0.010 (1)	0.008 (1)
O'2	0.128 (5)	0.146 (6)	0.055 (5)	0.092 (4)	0.045 (4)	0.042 (5)
O'1	0.091 (6)	0.033 (4)	0.073 (6)	0.007 (4)	0.000 (5)	0.001 (4)
N'2	0.056 (5)	0.054 (5)	0.110 (8)	0.021 (4)	0.033 (6)	0.032 (5)
N'1	0.076 (6)	0.058 (5)	0.048 (6)	0.032 (4)	0.006 (5)	0.007 (5)
C'2	0.045 (6)	0.086 (6)	0.096 (8)	0.038 (4)	0.036 (6)	0.064 (6)
C'1	0.075 (7)	0.054 (6)	0.051 (7)	0.036 (5)	0.015 (6)	0.024 (5)
C'4	0.057 (6)	0.048 (6)	0.072 (8)	0.022 (5)	0.025 (6)	0.021 (6)
C'3	0.059 (7)	0.044 (6)	0.026 (6)	0.011 (5)	0.000 (6)	0.009 (5)

(b) Final Isotropic Thermal Parameters for 2b

atom	$B, \text{\AA}^2$	atom	$B, \text{\AA}^2$	atom	$B, \text{\AA}^2$
C5	6.9 (4)	C1C	3.9 (3)	C'1B	4.6 (3)
C6	8.3 (5)	C2C	5.6 (3)	C'2B	7.6 (4)
C7	6.4 (4)	C3C	4.6 (3)	C'3B	7.2 (4)
C8	10.3 (6)	C4C	5.9 (4)	C'4B	5.9 (4)
C9	5.2 (3)	C5C	5.8 (3)	C'5B	5.3 (3)
C10	6.3 (4)	C6C	4.5 (3)	C'6B	6.4 (4)
C11	5.7 (3)	C'5	7.8 (4)	C'1C	3.8 (3)
C12	7.9 (4)	C'6	10.8 (6)	C'2C	4.3 (3)
C1A	5.2 (3)	C'7	6.2 (4)	C'3C	5.3 (3)
C2A	5.8 (3)	C'8	10.1 (5)	C'4C	5.3 (3)
C3A	5.8 (3)	C'9	6.3 (4)	C'5C	5.8 (3)
C4A	5.8 (3)	C'10	8.9 (5)	C'6C	4.9 (3)
C5A	4.0 (3)	C'11	7.1 (4)	C''1	18.2 (0)
C6A	3.5 (3)	C'12	9.4 (5)	C''2	11.7 (0)
C1B	4.2 (3)	C'1A	3.3 (3)	C''3	15.6 (0)
C2B	5.3 (3)	C'2A	4.6 (3)	C''4	20.1 (0)
C3B	4.0 (3)	C'3A	6.2 (4)	C''5	11.9 (0)
C4B	5.5 (3)	C'4A	6.3 (4)	C''6	13.3 (0)
C5B	5.6 (3)	C'5A	5.4 (3)	C''7	19.8 (0)
C6B	5.2 (3)	C'6A	4.3 (3)		

^a The form of the anisotropic temperature factor is $\exp[-2\pi^2(U_{11}h^2a^{*2} + U_{22}k^2b^{*2} + U_{33}l^2c^{*2} + 2U_{12}hka^*b^* + 2U_{13}hla^*c^* + 2U_{23}k lb^*c^*)]$.

of solvation in the asymmetric unit of the triclinic unit cell. The contents of the unit cell are shown in Figure 2. The structures of the two independent tungsten(II) complexes are essentially the same with analogous metal-to-ligand bond distances differing by less than 0.02 Å, analogous intraligand distances within 0.05 Å of one another, and intramolecular bond angles that correspond to within 2°. The atomic labeling scheme chosen for the two independent molecules is identical except that the chemical symbols for one are denoted with a prime. Intramolecular bond distances and angles are presented in Tables V and VI, respectively. Table VII lists pertinent least-squares planes coordinates, and Table VIII reports selected dihedral angles between several planes, each defined by three or more ligating atoms.

The solid-state structure of **2b** confirms the heptacoordinate nature of the central tungsten(II) ion in this complex. Both dithiocarbamate ligands are bidentate with the triphenylphosphine and both carbonyl ligands located mutually cis to one another. The following structural description will employ average parameter

values from the two independent molecules in order to facilitate the discussion.

The dithiocarbamate ligands exhibit normal geometries with each S_2CNC_2 unit essentially planar (within $<0.1 \text{ \AA}$).²³ The average C–N bond length of 1.32 Å indicates considerable double-bond character as is typical for chelated 1,1-dithiolate ligands. The observed chelate bites of 2.85 and 2.89 Å and bite angles of 68.7 and 69.0° for S1–S2 and S3–S4, respectively, and average W–S bond length of 2.54 Å are comparable to values observed for other (dithiocarbamate)tungsten complexes.^{11,24} The range

(23) (a) Coucouvanis, D. *Prog. Inorg. Chem.* **1979**, *26*, 301. (b) Bruder, A. H.; Fay, R. C.; Lewis, D. F.; Saylor, A. A. *J. Am. Chem. Soc.* **1976**, *98*, 6932. (c) Given, K. W.; Mattson, B. M.; Pignolet, L. H. *Inorg. Chem.* **1976**, *15*, 3152.

(24) (a) Butler, G.; Chatt, J.; Leigh, G. J.; Smith, A. R. P.; Williams, G. *A. Inorg. Chim. Acta* **1978**, *28*, L165. (b) Wijnhoven, J. G. *Cryst. Struct. Commun.* **1973**, *2*, 637. (c) Bino, A.; Cotton, F. A.; Dori, Z.; Sekutowski, J. C. *Inorg. Chem.* **1978**, *17*, 2946.

Table IV. $W(CO)_2L(S_2CNR_2)_2$ Carbon Monoxide Vibrational Data

complex	ν_{CO} , cm ⁻¹	medium	k_{CO} , ^a mdyn A ⁻¹	k_b , mdyn A ⁻¹	ref
1a	2020 1944 1926	toluene	15.57	0.45	14
1b	2005 1923 1905	toluene	15.27	0.48	11
$W(CO)_3[S_2CN(CH_2Ph)_2]_2$	2020 1931 1911	toluene	15.43	0.52	11
$W(CO)_3[S_2CN(CH_2)_5]_2$	2018 1927 1908	toluene	15.36	0.54	11
$W(CO)_2[S_2CNMe_2]_2$	1930 1803	Nujol	14.08	0.96	14
2a	1909 1821	Nujol	14.05	0.66	this work
2b	1920 1829	Nujol	14.20	0.69	this work
3a	1945 1847	Nujol	14.52	0.75	this work
3b	1930 1838	CH ₂ Cl ₂	14.34	0.70	this work
4a	1917 1818	Nujol	14.09	0.75	this work
4b	1915 1825	Nujol	14.13	0.68	this work
5b	1923 1830	toluene	14.23	0.70	this work

^a These approximate force constants are derived on the basis of assumptions discussed in the text.

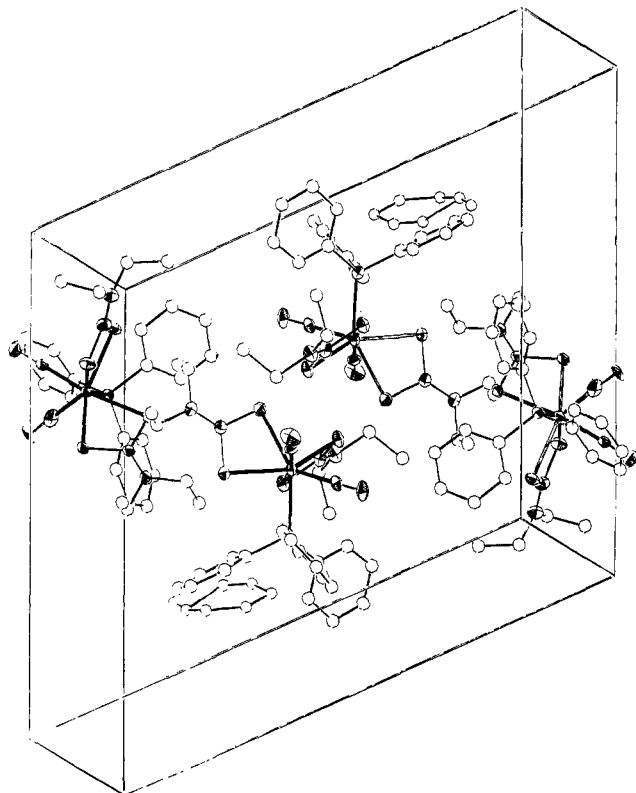


Figure 2. A view of the unit cell contents of **2b** with *a* horizontal, *b* nearly vertical, and *c* perpendicular to the plane of the paper with the unit cell origin in the rear lower left-hand corner.

of W-S distances for **2b** (2.49–2.56 Å) parallels the metal-sulfur bond lengths of **1a** (2.50–2.57 Å).¹¹

The average W-C bond length of 1.97 Å is typical for tungsten-carbonyl derivatives.²⁵ No significant distinction between

Table V. Intramolecular Bond Distances (Å) for **2b**

A. Tungsten Coordination Sphere			
W-S4	2.562 (3)	W'-S'4	2.548 (3)
W-S3	2.530 (3)	W'-S'3	2.544 (3)
W-S2	2.550 (3)	W'-S'2	2.556 (3)
W-S1	2.496 (3)	W'-S'1	2.487 (3)
W-C2	1.978 (13)	W'-C'2	1.964 (13)
W-C1	1.939 (13)	W'-C'1	1.977 (13)
W-P	2.490 (3)	W'-P'	2.480 (3)
B. <i>N,N</i> -Diethyldithiocarbamate and Carbon Monoxide Ligands			
C2-O2	1.148 (11)	C'2-O'2	1.142 (13)
C1-O1	1.161 (11)	C'1-O'1	1.158 (11)
S4-C4	1.718 (11)	S'4-C'4	1.710 (10)
S3-C4	1.714 (11)	S'3-C'4	1.713 (11)
S2-C3	1.700 (10)	S'2-C'3	1.686 (10)
S1-C3	1.724 (10)	S'1-C'3	1.731 (10)
C4-N2	1.320 (12)	C'4-N'2	1.315 (12)
C3-N1	1.329 (12)	C'3-N'1	1.334 (11)
N2-C9	1.501 (14)	N'2-C'9	1.553 (15)
N2-C11	1.498 (14)	N'2-C'11	1.532 (13)
N1-C5	1.479 (14)	N'1-C'5	1.508 (13)
N1-C7	1.510 (13)	N'1-C'7	1.500 (14)
C9-C10	1.501 (17)	C'9-C'10	1.439 (19)
C11-C12	1.529 (18)	C'11-C'12	1.494 (18)
C5-C6	1.555 (15)	C'5-C'6	1.533 (17)
C7-C8	1.513 (16)	C'7-C'8	1.523 (18)
C Triphenylphosphine Ligands			
P-C1A	1.837 (11)	P'-C'1A	1.818 (10)
P-C1B	1.844 (10)	P'-C'1B	1.855 (11)
P-C1C	1.828 (10)	P'-C'1C	1.826 (10)
C1-A-C2A	1.42 (2)	C'1A-C'2A	1.39 (1)
C2A-C3A	1.42 (2)	C'2A-C'3A	1.43 (1)
C3A-C4A	1.38 (2)	C'3A-C'4A	1.44 (2)
C4A-C5A	1.39 (2)	C'4A-C'5A	1.40 (2)
C5A-C6A	1.43 (1)	C'5A-C'6A	1.42 (1)
C6A-C1A	1.39 (1)	C'6A-C'1A	1.40 (1)
C1B-C2B	1.41 (2)	C'1B-C'2B	1.40 (1)
C2B-C3B	1.44 (2)	C'2B-C'3B	1.39 (2)
C3B-C4B	1.34 (2)	C'3B-C'4B	1.38 (2)
C4B-C5B	1.39 (1)	C'4B-C'5B	1.40 (1)
C5B-C6B	1.48 (1)	C'5B-C'6B	1.46 (2)
C6B-C1B	1.41 (2)	C'6B-C'1B	1.39 (2)
C1C-C2C	1.38 (1)	C'1C-C'2C	1.40 (1)
C2C-C3C	1.43 (1)	C'2C-C'3C	1.42 (1)
C3C-C4C	1.40 (1)	C'3C-C'4C	1.39 (1)
C4C-C5C	1.38 (1)	C'4C-C'5C	1.39 (1)
C5C-C6C	1.46 (1)	C'5C-C'6C	1.41 (1)
C6C-C1C	1.40 (1)	C'6C-C'1C	1.39 (1)

C1 and C2 is possible solely on the basis of observed bond lengths. Furthermore the carbon position of a carbon monoxide ligand bound to a heavy-metal often is poorly refined compared to the terminal oxygen atom,²⁶ and here the W-O distances reinforce the above conclusion by averaging 3.12 Å for both W-O1 and W-O2.

The W-P bond distance of 2.49 Å is among the lower values reported for tungsten(II)-carbonyl-phosphine complexes (generally between 2.5 and 2.6 Å).²⁷ Note that three closely related complexes recently reported by Archer and co-workers also display W-P distances of 2.48–2.50 Å.²⁸ Longer tungsten-phosphorus bond distances, near 2.6 Å, are generally found in complexes where the high trans influence of carbon monoxide may play a role in determining the W-P length.²⁷ The cis orientation of triphenylphosphine and the two carbonyl ligands in **2b** (P-W-C angles of 73.8 and 106.5°) indicates that the carbon monoxide trans influence will not be an important factor in considering the metal-phosphine bond in **2b** in accord with the relatively short

(25) Drew, M. G. B.; Rix, C. J. *J. Organomet. Chem.* **1975**, *102*, 467.

(26) (a) Goldberg, S. Z.; Raymond, K. N. *Inorg. Chem.* **1973**, *12*, 2923.

(b) Mawby, A.; Pringle, G. E. *J. Inorg. Nucl. Chem.* **1972**, *34*, 517.

(27) (a) Drew, M. G. B.; Tomkins, I. B.; Colton, R. *Aust. J. Chem.* **1970**, *23*, 2517. (b) Churchill, M. R.; Youngs, W. J. *Inorg. Chem.* **1979**, *18*, 2454.

(28) Day, R. O.; Batschelet, W. H.; Archer, R. D. *Inorg. Chem.* **1980**, *19*, 2113.

Table VI. Intramolecular Bond Angles (Deg) for 2b

A. Tungsten Coordination Sphere Angles			
S4-W-S3	69.18 (9)	S'4-W'-S'3	68.88 (9)
S4-W-S2	86.41 (10)	S'4-W'-S'2	85.50 (10)
S4-W-S1	80.24 (9)	S'4-W'-S'1	79.40 (9)
S4-W-P	151.18 (9)	S'4-W'-P'	149.21 (9)
S3-W-S2	87.48 (9)	S'3-W'-S'2	92.26 (9)
S3-W-S1	142.54 (9)	S'3-W'-S'1	144.15 (9)
S3-W-P	83.44 (9)	S'3-W'-P'	82.56 (9)
S2-W-S1	69.01 (8)	S'2-W'-S'1	68.38 (9)
S2-W-P	83.49 (9)	S'2-W'-P'	84.34 (9)
S1-W-P	120.40 (9)	S'1-W'-P'	122.85 (9)
S4-W-C2	79.4 (3)	S'4-W'-C'2	81.8 (3)
S4-W-C1	133.7 (3)	S'4-W'-C'1	135.7 (3)
S3-W-C2	84.0 (3)	S'3-W'-C'2	81.5 (3)
S3-W-C1	139.2 (3)	S'3-W'-C'1	137.2 (3)
S2-W-C2	165.4 (3)	S'2-W'-C'2	167.2 (3)
S2-W-C1	121.9 (3)	S'2-W'-C'1	119.5 (3)
S1-W-C2	111.8 (3)	S'1-W'-C'2	110.8 (3)
S1-W-C1	78.0 (3)	S'1-W'-C'1	77.8 (3)
P-W-C2	107.2 (3)	P'-W'-C'2	105.7 (3)
P-W-C1	73.7 (3)	P'-W'-C'1	73.8 (3)
C2-W-C1	71.6 (4)	C'2-W'-C'1	71.7 (4)
B. Ligating Atom Angles			
W-C2-O2	178.1 (1.0)	W'-C'2-O'2	179.8 (1.5)
W-C1-O1	173.2 (1.0)	W'-C'1-O'1	175.3 (1.0)
W-P-C1A	113.4 (4)	W'-P'-C'1A	113.3 (3)
W-P-C1B	114.1 (3)	W'-P'-C'1B	116.1 (3)
W-P-C1C	117.1 (3)	W'-P'-C'1C	116.4 (3)
W-S4-C4	87.2 (4)	W'-S'4-C'4	88.0 (4)
W-S3-C4	88.3 (4)	W'-S'3-C'4	88.1 (4)
W-S2-C3	88.3 (4)	W'-S'2-C'3	89.1 (4)
W-S1-C3	89.5 (4)	W'-S'1-C'3	90.4 (4)
C. N,N-Diethyldithiocarbamate Angles			
S4-C4-S3	114.8 (6)	S'4-C'4-S'3	114.6 (7)
S2-C3-S1	113.2 (6)	S'2-C'3-S'1	112.1 (6)
S4-C4-N2	122.6 (9)	S'4-C'4-N'2	122.6 (8)
S3-C4-N2	122.6 (8)	S'3-C'4-N'2	122.8 (8)
S2-C3-N1	124.6 (8)	S'2-C'3-N'1	125.1 (8)
S1-C3-N1	122.2 (8)	S'1-C'3-N'1	122.8 (8)
C4-N2-C9	121.6 (9)	C'4-N'2-C'9	122.5 (9)
C4-N2-C11	120.7 (9)	C'4-N'2-C'11	122.3 (9)
C3-N1-C5	122.3 (8)	C'3-N'1-C'5	120.4 (9)
C3-N1-C7	120.5 (8)	C'3-N'1-C'7	120.5 (9)
N2-C9-C10	108.5 (1.0)	N'2-C'9-C'10	105.1 (1.2)
N2-C11-C12	107.1 (1.0)	N'2-C'11-C'12	109.4 (1.0)
N1-C5-C6	109.8 (9)	N'1-C'5-C'6	109.5 (1.0)
N1-C7-C8	110.1 (9)	N'1-C'7-C'8	106.9 (1.0)

distance observed. The phenyl rings of the phosphine ligand do not appear to place significant steric constraints on the coordination geometry at the metal center. The dithiocarbamate ethyl substituents are crystallographically well-behaved.

The geometry of the inner coordination sphere for seven-coordinate monomers can be analyzed by measuring dihedral angles (δ_i) between triangular faces defined by ligating atoms either before^{10,29} or after³⁰ normalization of the metal-ligand bond distances. Of the seven ligating atoms, least-squares planes calculations identified only one group of four (S1S2PC1) which approximates a plane (average deviation of 0.09 Å, see Table VII). Quantitative analysis of the parent tricarbonyl structure **1a** led us to choose the tetragonal base-trigonal base (4:3) geometry as the most informative and accurate idealized seven-coordinate description in that case.¹¹ The planarity of four cis ligands in **2b** suggested that the most lucid comparison of **2b** with **1a** would follow from a 4:3 description of **2b**, utilizing normalized metal-ligand bond lengths. When viewed as a 4:3 geometry, necessarily defined by the distribution S1S2PC1:S3S4C2, the 4:3 dihedral angle (based on unit bond lengths) of 1.5° (13.4° without normalization) compares favorably with the idealized value of 0°. The planarity of the quadrilateral face can be assessed not only

Table VII. Least-Squares Planes for 2b

A. Observed Orthogonal Atomic Coordinates				
atom	x	y	z	
S1	-1.674	8.902	-0.915	
S2	-0.502	6.519	0.146	
S3	2.712	7.857	0.612	
S4	1.434	8.634	-1.861	
C1	-0.642	10.269	1.331	
C2	1.395	10.586	0.330	
P	0.301	8.282	2.886	
Constants for the Planes Equations ^a				
atoms defining the plane	A	B	C	D
S1 S2 C1 P	0.886	0.175	-0.429	0.558
S3 S4 C2	0.864	0.383	-0.326	5.155
S1 S4 C2	-0.137	0.738	-0.660	7.408
S1 C1 C2	-0.322	0.867	-0.379	8.607
S2 S3 S4	0.497	-0.796	-0.456	-5.458
S2 S3 P	-0.284	0.842	-0.458	5.566
S1 S2 C1	0.843	0.191	-0.503	0.746
S2 C1 P	0.919	0.150	-0.366	0.463
S3 C1 C2	-0.388	-0.278	-0.879	-3.774
S3 C1 P	-0.576	-0.656	-0.489	-7.011
S3 C2 P	-0.667	-0.387	-0.636	-5.245
C1 C2 P	-0.242	-0.666	-0.705	-7.627
S1 S2 S4	-0.291	-0.505	-0.813	-3.263
S1 S2 P	0.876	0.246	-0.415	1.104
S1 C1 P	0.890	0.070	-0.451	-0.457
B. Normalized Orthogonal Atomic Coordinates ^b				
atom	x	y	z	
S1	-0.429	8.889	-0.084	
S2	0.047	7.956	0.343	
S3	1.314	8.476	0.527	
S4	0.804	8.785	-0.440	
C1	-0.138	9.597	0.914	
C2	0.924	9.702	0.399	
P	0.361	8.640	1.441	
Constants for the Planes Equations ^a				
atoms defining the plane	A	B	C	D
S1 S2 C1 P	0.877	0.243	-0.414	1.825
S3 S4 C2	0.887	0.242	-0.391	3.013
S1 S4 C2	-0.151	0.678	-0.719	6.155
S1 C1 C2	-0.316	0.815	-0.486	7.418
S2 S3 S4	0.394	-0.794	-0.462	-6.459
S2 S3 P	-0.284	0.848	-0.448	6.575
S1 S2 C1	0.870	0.247	-0.428	1.857
S2 C1 P	0.883	0.239	-0.403	1.810
S3 C1 C2	-0.408	-0.222	-0.886	-2.885
S3 C1 P	-0.604	-0.602	-0.522	-6.174
S3 C2 P	-0.688	-0.288	-0.666	-3.701
C1 C2 P	-0.310	-0.577	-0.756	-6.187
S1 S2 S4	-0.278	-0.513	-0.813	-4.369
S1 S2 P	0.845	0.257	-0.411	1.942
S1 C1 P	0.879	0.229	-0.418	1.696

^a The equation for each plane is of the form $Ax + By + Cz = D$.

^b These values are calculated by normalization of all seven M-L bond distances as discussed in the text.

by the average deviation (vide supra) but also from the dihedral angle (δ) between two triangular components of the four quadrilateral vertices. For **2b** a δ value of 1.7° (9.3° unnormalized) indicates the validity of the tetragonal base description for atoms S1S2PC1.

A projection of the normalized inner coordination sphere, observed from above the quadrilateral face, is presented in Figure 3. This view emphasizes the eclipsed orientation of C1 and C2 with S3 and S4 of the trigonal plane roughly bisecting the PS2 and S1S2 quadrilateral edges, respectively.

Comparison of the molecular geometries of **1a** and **2b** reveals a remarkable consistency in the inner coordination sphere. In fact the naive presumption that substitution of a single π -acceptor

(29) Porai-Koshits, M. A.; Aslanov, L. A. *Zh. Strukt. Khim.* **1972**, *13*, 266.

(30) Kouba, J. K.; Wreford, S. S. *Inorg. Chem.* **1976**, *15*, 1463.

Table VIII. Dihedral Angle Calculations for Comparison of 2b with Idealized Geometries^a

trial geometry	defining planes	δ_i	δ_i		
			obsd	normalzd ^b	idealzd
4:3 (piano stool)	S1 S2 C1 P/S3 S4 C2	δ_1	13.4	1.4	0.0
C1PS1S2:C2S3S4	S1 S2 P/C1 S1 P	δ_2	10.4	1.7	0.0
1:4:2 (capped trigonal prism)	S1 S4 C2/S1 C1 C2	δ_1	20.7	18.2	41.5
CTP-1, S4:C2S1S2S3:PC1	S2 S3 S4/S2 S3 P ^c	δ_1'	54.9	54.7	41.5
	S1 S2 C1/S2 C1 P	δ_2	9.3	1.7	0.0
	S3 C1 C2/S3 C1 P	δ_3	33.4	32.6	0.0
1:4:2 (capped trigonal prism)	S3 C2 (P)/C1 C2 P	δ_1	29.7	28.0	41.5
CTP-2, S3:C2PS2S4:S1C1	S2 C3 S4/S1 S2 S4 ^c	δ_1'	49.0	47.7	41.5
	S1 S4 C2/S1 C1 C2	δ_2	20.7	18.2	0.0
	S1 S2 P/S1 C1 P	δ_3	10.4	1.6	0.0

^a See text for references to the idealized geometries and the corresponding δ_i values. ^b These dihedral angles were calculated following projection of the ligating atoms onto a sphere of unit radius. ^c The δ_1' values represent an alternate, but equally valid, choice of planes to define δ_1 .

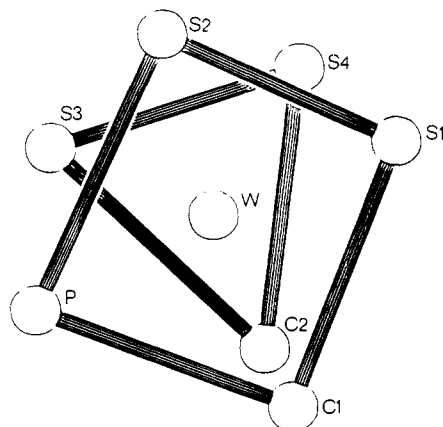


Figure 3. A view of a projection of the inner coordination sphere of 2b onto a sphere of unit radius illustrating the 4:3 "piano stool" geometry. The view is from above the quadrilateral plane.

carbonyl ligand by the bulky triphenylphosphine donor would occur with retention of the inner coordination sphere geometry with the incoming ligand simply occupying one of the original three carbonyl sites proves surprisingly accurate. Certainly extensive rearrangement of the seven donor sites as a result of the substitution would not have been considered unusual. The atoms of 2b have been labeled to facilitate correlation of the ligating atoms in the 1:1 manner indicated in Table IX. The proximity of corresponding interligand angles illuminates the striking structural relationship between $W(CO)_3(S_2CNMe_2)_2$ and $W(CO)_2(PPh_3)(S_2CNEt_2)_2$. Metal-ligand bond distances also reflect the structural commonality of 1a and 2b with the obvious exception of W-C3 of 1a vs. W-P of 2b. The close correspondence observed for these seven-coordinate complexes in the solid state suggests that one might profitably seek similarities between the solution behavior of the two complexes as well (vide infra).

Alternative descriptions of the observed structure of 2b can be based on one of the three common idealized seven-coordinate polyhedra (D_{3h} , 1:5:1; C_{3v} , 1:3:3; C_{2v} , 1:4:2). A capped trigonal prism, C_{2v} -S4:C2S1S2S3:C1P, can be easily derived from the 4:3 description suggested above in accord with guidelines presented by Drew.^{8a} Even for the capped trigonal prism (CTP) geometry the correspondence of ligands and positions is not unique, and for 2b comparable agreement with idealized δ values is generated with S3 as the capping ligand. The normalized coordination sphere δ_i calculations for the 4:3 and both CTP choices are included in Table VIII for 2b. Although the δ_i angles characterizing the two CTP alternatives for 2b are not as near the idealized angles as those calculated for the 4:3 model, the correlation between observed and idealized dihedral angles makes either CTP a possible, though less preferable, option. Furthermore the average δ_1 values of 36.5° (18.2 and 54.7) and 37.9 (28.0 and 47.7) for CTP-1 and CTP-2 approach the theoretical angle of 41.5° associated with an undistorted CTP geometry and compare favorably with related dihedral angles calculated for other monomeric 1:4:2 complexes.³¹

Table IX. Coordination Sphere Comparisons for 1a and 2b

	Bond Distances (Å)	
	$W(CO)_3[S_2CNMe_2]_2$ (1a)	$W(CO)_2(PPh_3)[S_2CNEt_2]_2$ (2b)
W-S1	2.50	2.50
W-S2	2.54	2.55
W-S3	2.52	2.53
W-S4	2.57	2.56
W-C1	1.96	1.94
W-C2	2.02	1.98
W-C3(P)	1.97	2.49
	Bond Angles (Deg)	
	$W(CO)_3[S_2CNMe_2]_2$ (1a)	$W(CO)_2(PPh_3)[S_2CNEt_2]_2$ (2b)
S1-W-S2	69.1	69.0
S1-W-S3	146.3	142.5
S1-W-S4	81.3	80.2
S1-W-C1	78.8	78.0
S1-W-C2	110.7	111.8
S1-W-C3(P)	122.0	120.4
S2-W-S3	92.6	87.5
S2-W-S4	86.1	86.4
S2-W-C1	118.1	121.9
S2-W-C2	166.4	165.4
S2-W-C3(P)	82.4	83.5
S3-W-S4	69.0	69.2
S3-W-C1	134.6	139.2
S3-W-C2	80.6	84.0
S3-W-C3(P)	80.9	83.4
S4-W-C1	139.7	133.7
S4-W-C2	80.5	79.4
S4-W-C3(P)	147.3	151.2
C1-W-C2	74.4	71.6
C1-W-C3(P)	71.7	73.7
C1-W-C3(P)	107.8	107.2

The large differences (36.5 and 19.7°) observed for the two alternative choices of δ_1 in each CTP case reflect the constraint of the dithiocarbamate bite which prohibits the capping S atom from residing in the center of the quadrilateral face.

NMR Properties of $W(CO)_2L(S_2CNR_2)_2$ Complexes. Pertinent chemical shifts (³¹P and ¹³C) and coupling constants for complexes 2, 3, 4 and 5 are listed in Table X with data for the parent tricarbonyl compound, 1, included for purposes of comparison. The ³¹P shifts observed are typical for these ligands bound to tungsten.³²

The average carbon-13 chemical shift for the two carbonyl ligands in $W(CO)_2L(S_2CNR_2)_2$ complexes is approximately 15

(31) (a) Lewis, D. F.; Lippard, S. J. *Inorg. Chem.* **1972**, *11*, 621. (b) Drew, M. G. B.; Wilkins, J. D. *J. Organomet. Chem.* **1974**, *69*, 271. (c) Cradwick, E. M.; Hall, D. *Ibid.* **1970**, *25*, 91. (d) Drew, M. G. B. *J. Chem. Soc., Dalton Trans.* **1972**, 626. (e) Drew, M. G. B.; Wilkins, J. D. *Ibid.* **1974**, 1654.

(32) Pregosin, P. S.; Kunz, R. W., "NMR Basic Principles and Progress"; Springer Verlag: New York, 1979; Vol. 16 and references contained therein.

Table X. Carbon-13 NMR Data and Selected Coupling Constants^a

compd	$\delta(^{13}CO)^b$	$^1J_{^{183}W-^{13}C}$	$^1J_{^{183}W-^{31}P}$	$^2J_{^{13}C-W-^{31}P}$
1a	218.2			
	233.2			
	248.8			
1b	218.7	133		
	234.2	133		
	249.7	91		
2a	233.2			
	268.2			
2b	232.9	147	222	7
	269.9	105		34
3b	229.2	145	334	15
	265.4	105		45
4a			216	
4b			220	
5b	233.4	153	219	6
	269.9	105		32

^a Chemical shifts are in ppm relative to Me_4Si and coupling constants are in Hz. ^b Low-temperature limiting spectra were the source of the δ values listed.

ppm below the average carbonyl shift of the tricarbonyl compounds, **1a** and **1b**. A downfield shift is commonly observed for carbonyl ligands remaining in the coordination sphere when a phosphorus donor replaces carbon monoxide.³³ Decreased competition for the available metal $d\pi$ electron density is considered to play a role in determining the carbon-13 chemical shift. Literature precedent suggests that the difference in carbon-13 shifts for cis and trans carbonyls in substituted octahedral complexes is considerably less than the downfield shift experienced by both types of carbonyl ligands in the substituted complex relative to the starting carbonyl material.³⁴ These observations provide a basis for the hypothesis that the two carbonyls remaining in the tungsten coordination sphere for $W(CO)_2L(S_2CNR_2)_2$ complexes will shift downfield by roughly equal amounts. This argument is particularly credible where both carbon monoxide ligands are cis to the incoming ligand, as is the case for **2b**. This analysis leads one to conclude that the carbonyl ligand with the lowest chemical shift (249 ppm) in **1a** moves downfield to about 268 ± 3 ppm in $W(CO)_2L(S_2CNR_2)_2$ complexes while the upfield carbonyl of **1a** (218 ppm) drops to 232 ± 3 ppm. Only the **1a** carbonyl with an original shift of 233 ppm is not retained in the substituted derivatives since, even considering a possible downfield shift range of anywhere from 10 to 30 ppm, there is no carbon-13 resonance in the appropriate region (243–263 ppm). This series of logical assumptions allows one to assign the 233-ppm ^{13}C signal to **1a** to C_3 with a high degree of confidence. Alternative assignments for this central carbonyl signal would require either no change in the carbon-13 chemical shift when a phosphine replaces an adjacent carbonyl or a shift of more than 30 ppm downfield.

The remaining two carbonyl signals of **1a** can be assigned on the basis of the established π -donor capability of dithiocarbamate ligands^{12a,35} and the location of the sulfur atoms relative to the bound carbon nuclei. Since carbonyl ligands which are trans to ligands with no π -acceptor qualities tend to exhibit lower field carbon-13 chemical shifts than those that are cis to such ligands³⁶ an effort to assign the low field signals of **1** and **2** should seek the carbonyl most nearly trans to a sulfur. Indeed a single carbonyl-sulfur pair, namely, C_2-S_2 , is substantially closer to a trans arrangement (166.4° (**1a**) and 165.4° (**2b**)) in both structures

than any other pair. If one assigns C_2 to the low field carbon-13 signal on the basis of the π -donor character of S_2 (this is consistent with the previous assignment of **1a** predicated on an analysis of the dynamic behavior exhibited by the tricarbonyl fragment) and C_3 is assigned as above, then C_1 must necessarily correspond to the 218-ppm signal of **1a** and to the signal near 232 ppm in the $W(CO)_2L(S_2CNR_2)_2$ complexes.

The above assignments for C_1 and C_3 in **1a** are also compatible with expectations based on observed $C-W-S$ angles of 147.3° and 139.7° for C_3-W-S_4 and C_1-W-S_4 , respectively, since the larger angle corresponds to the lower chemical shift. An additional feature of this model is that C_2 is 107.2° from P in **2b** and shifts downfield by 21 ppm, cf. C_2 of **1a**, while C_1 is 73.7° away and shifts by 15 ppm in accord with rational expectations for the effect of mutually cis carbonyls with one angle larger than the other. In summary it remains true that these assignments must be viewed as tentative, but they provide a working model which appears to be consistent with the available data. Rational assignment of the three unique carbonyl resonances exhibited by **1a** is a substantial accomplishment.

One bond $^1J_{^{183}W-^{31}P}$ (^{183}W , 14.42%) coupling constants are in the normal range for tungsten-phosphine complexes (see Table X).³⁷ The triethyl phosphite complex **3b** exhibits a metal-phosphorus coupling constant about 50% larger than the phosphine complexes in accord with a large body of literature data for $M-P(OR)_3$ compared to $M-PR_3$.³⁸

One bond $^1J_{^{183}W-^{13}C}$ coupling constants for **2b**, **3b**, and **5b** proved informative. In each of these three complexes there is a difference of 40–50% between tungsten coupling to each of the two carbonyl ligands. In each instance it is the low-field signal which shows the smaller coupling (105 Hz) while the upfield signal is split by the NMR-active metal nucleus to a much greater extent (145–153 Hz). The magnitude of the variance between the two coupling constants is unusually large for two carbonyls in the same tungsten complex; typical cis and trans $^1J_{W-C}$ values for $LW(CO)_2$ complexes fall near 120 and 140 Hz, respectively.³⁹ The Fermi contact term, and hence mutual s character from both nuclei present in specific molecular orbitals, generally determines the magnitude of one-bond coupling constants.⁴⁰ Simple symmetry considerations exclude s orbitals from involvement in retrodative π bonding from metal $d\pi$ to carbonyl π^* orbitals, and therefore $^1J_{W-C}$ will be independent, to first order, of the extent of back-bonding.

Two bond coupling constants involving metal-bound ^{31}P and ^{13}C nuclei reinforce the NMR distinction between the two carbonyl ligands. In spite of the relative cis orientation of the phosphine donor to both carbon monoxide ligands a multiplicative factor of from 3 to 5 distinguishes the magnitude of the two $^2J_{P-W-C}$ values. For **2b** the coupling constants of 7 and 34 Hz presumably reflect the solid-state geometry where $P-W-C$ angles of 73.7 and 107.2° are found to C_1 and C_2 , respectively. Although the differing magnitudes of two-bond coupling constants for cis and trans ligand orientations have been extensively documented empirically (and can be readily rationalized for octahedral complexes),^{36,41} the case in question is not readily amenable to a similar analysis. The deviation of the $P-W-C$ angle from 90° is -16.3 and $+17.2^\circ$ for C_1 and C_2 , respectively, and there is no apodictical basis for correlating the larger angle with the larger coupling constant. On the basis of the carbonyl carbon-13 assignments discussed above, the 34-Hz coupling would in fact correspond to the obtuse $P-W-C_2$ angle since it is associated with the low-field ^{13}C resonance tentatively assigned as C_2 . It may be possible to definitively assign these $^2J_{^{31}P-W-^{13}C}$ coupling constants by analogy if low-temperature carbon-13 data can be resolved for the seven coordinate tungsten

(33) (a) Cotton, F. A.; Lahuerta, P.; Stults, B. R. *Inorg. Chem.* **1976**, *15*, 1866. (b) Cotton, F. A.; Hunter, D. L. *J. Am. Chem. Soc.* **1975**, *97*, 5739. (c) Bodner, G. M.; Todd, L. J. *Inorg. Chem.* **1974**, *13*, 1335.

(34) Todd, L. J.; Wilkinson, J. R. *J. Organomet. Chem.* **1974**, *77*, 1 and references contained therein.

(35) (a) Coucouvanis, D. *Prog. Inorg. Chem.* **1970**, *11*, 233. (b) Bereman, R. D.; Naleajek, D. *Inorg. Chem.* **1977**, *16*, 2687. (c) Eisenberg, R. *Prog. Inorg. Chem.* **1970**, *12*, 295.

(36) (a) Mann, B. E. *J. Chem. Soc., Dalton Trans.* **1973**, 2012. (b) Braterman, P. S.; Milne, D. W.; Randall, E. W.; Rosenberg, E. *Ibid.* **1973**, 1027.

(37) Grim, S. O.; Wheatland, D. A.; McFarlane, W. *J. Am. Chem. Soc.* **1967**, *89*, 5573.

(38) Grim, S. O.; McAllister, P. R.; Singer, R. M. *J. Chem. Soc., Chem. Commun.* **1969**, 38.

(39) Mann, B. E. *Adv. Organomet. Chem.* **1974**, *12*, 135.

(40) (a) Pople, J. A.; Santry, D. P. *Mol. Phys.* **1964**, *8*, 1. (b) Jameson, C. J.; Gutowsky, H. S. *J. Chem. Phys.* **1969**, *51*, 2790.

(41) (a) Chisholm, M. H.; Godleski, S. *Prog. Inorg. Chem.* **1976**, *20*, 299.

(b) Gansow, O. A.; Kimura, B. Y.; Dobson, G. R.; Brown, R. A. *J. Am. Chem. Soc.* **1971**, *93*, 5922.

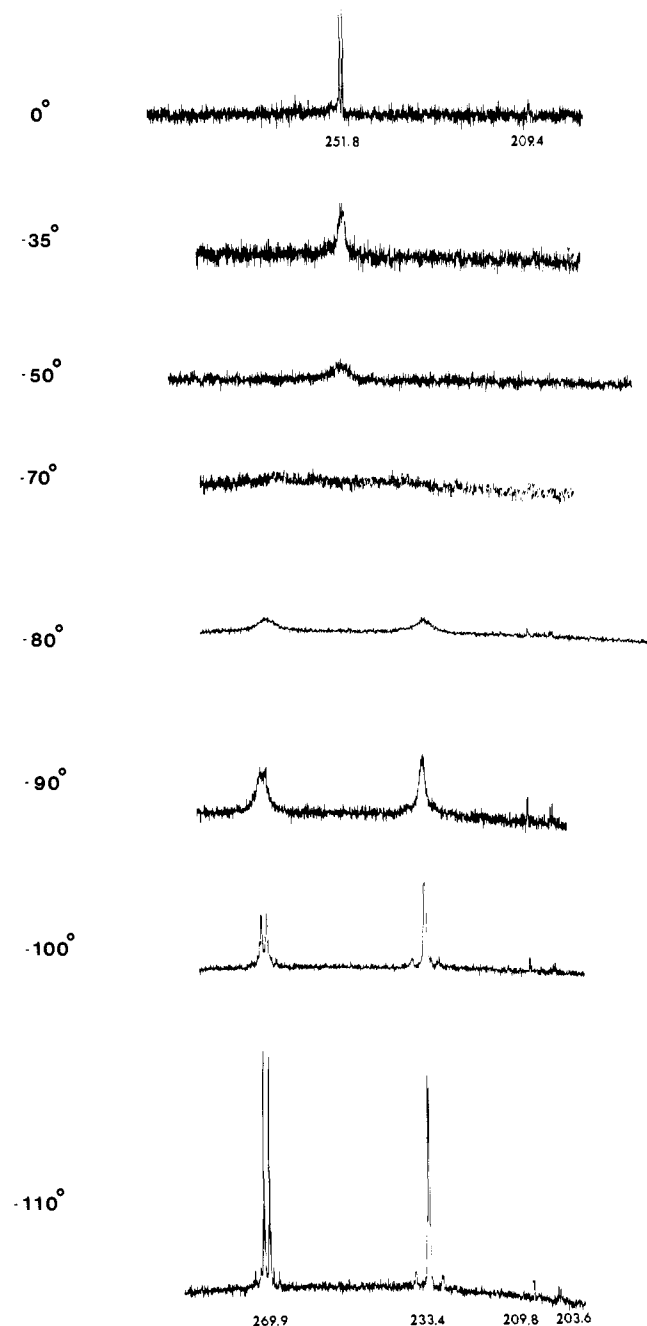


Figure 4. Variable-temperature $^{13}\text{C}\{^1\text{H}\}$ NMR spectra of ^{13}CO -enriched **5b** in the low-field region displaying resonances due to ^{13}CO and naturally abundant $\text{Et}_2\text{N}^{13}\text{CS}_2$ (chemical shifts are listed in ppm downfield from Me_4Si).

compounds recently reported by Day, Batschelet, and Archer where all the P–W–C angles are between 70° and 75° in the solid state.^{28,42}

Dynamic Properties of $\text{W}(\text{CO})_2\text{L}(\text{S}_2\text{CNR}_2)_2$ Complexes in Solution. The stereochemical nonrigidity of **2b**, **3b**, and **5b** was probed by variable-temperature carbon-13 NMR studies. The diethyldithiocarbamate derivatives were selected for study because of their solubility in the toluene-*d*₈-vinyl chloride (2:1) low temperature solvent (solvent mixtures containing CDCl_3 or CCl_4 led to decomposition). The availability of ^{13}CO -enriched **1b**¹⁴ for use as a reagent in preparing $\text{W}(^{13}\text{CO})_2\text{L}(\text{S}_2\text{CNR}_2)_2$ derivatives allowed us to obtain useful carbon-13 spectra from 0 to -110°C

(42) Carbon-13 NMR studies of $\text{W}(\text{CO})_2(\text{PPh}_3)_2(\text{dcq})\text{Cl}$, where all four P–W–C angles are between 72° and 78° in the solid state (see ref 28), exhibit an average $^2J_{\text{P-W-}^{13}\text{C}}$ coupling constant of 32 Hz at room temperature, thus confirming the coupling constant assignments proposed for **2b**. Archer, R. D.; Batschelet, W. H.; Nieter, S. J.; Templeton, J. L., unpublished results.

Table XI. Activation Barriers Calculated for $\text{W}(\text{CO})_2\text{L}(\text{S}_2\text{CNR}_2)_2$ Complexes^a

compd	ΔG^\ddagger , ^b kcal mol ⁻¹	temp range, $^\circ\text{C}$
2b	9.9 ± 0.1^c	-20 to -80
3b	8.0 ± 0.2	-70 to -100
5b	8.7 ± 0.1	-35 to -100
1a ^d	9.0 ± 0.1	-65 to -99
1b ^e	8.1 ± 0.1	-91 to -110
	8.5 ± 0.1	-30 to -90
	7.5 ± 0.1	-100 to -115

^a See text for details of the ΔG^\ddagger calculation. ^b Based on CO exchange as monitored by carbon-13 NMR. ^c The \pm values following ΔG^\ddagger serve only as an indication of the agreement for determinations at various temperatures and do not represent error limits. ^d Reference 14. ^e Reference 11.

where low-temperature limiting spectra were recorded for the unique carbonyl sites. An averaging of the two carbon monoxide ligand environments was observed with increasing temperature for each of the three complexes examined (see Figure 4). Seven-coordinate complexes are commonly nonrigid,⁵ and the dynamic behavior of these complexes is not unexpected.

Only a single ^{31}P resonance was present for **2b**, **3a**, **4a**, **4b**, and **5b**. No ^{31}P -exchange process was indicated by low-temperature spectra, suggesting that only one isomer is ever substantially populated in solution. In conjunction with the fluxional process evident in the carbon-13 spectra the phosphorous-31 NMR data are compatible with a molecular rearrangement which retains the ground-state structure while exchanging identical ligands between nonequivalent sites. Rearrangement processes to form distinct isomers with differing phosphorus environments in the metal coordination sphere were not detected.

The discussion which follows utilizes the observed solid-state geometry of **2b** as a model for interpreting the solution behavior of **2b** as reflected in NMR studies. As a precautionary note it should be added that the solid-state structure may not be the species present in solution, but in the absence of contradictory data it seems most feasible to assume similar structures in solution and in the solid.

The similarity of chemical shifts and coupling constants discussed above support the premise that **2b**, **3b**, and **5b**, and presumably related $\text{W}(\text{CO})_2(\text{PR}_3)(\text{S}_2\text{CNR}_2)_2$ derivatives, adopt essentially the same gross geometry in solution. Given the parallel spectral properties of these complexes, it seems reasonable to assume that essentially the same physical process is responsible for averaging the carbonyl environments in these three cases. The analysis which follows will focus on **2b** with the implicit assumption that similar rearrangements occur for the other complexes.

The single carbonyl resonance seen at 0°C broadens progressively upon cooling in a manner consistent with a simple two-site exchange process. Two well-resolved carbon-13 carbonyl ligand signals with a 1:1 intensity ratio are observed at -110°C . The single resonance attributable to the central dithiocarbamate carbon also broadens and separates into two distinct signals over this temperature range. Broadening is also observed for the dithiocarbamate alkyl carbons as the temperature is lowered, but separate resonances are not resolved at -110°C .

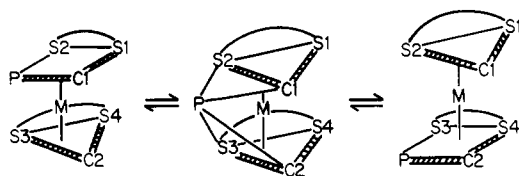
Activation barriers for this exchange process were calculated from the Eyring equation after k_{ex} was determined from the Gutowsky–Holm equation at the coalescence temperature⁴³ and the fast-and-slow-exchange approximations⁴⁴ were employed as discussed in detail previously.¹¹ The resulting ΔG^\ddagger values are listed in Table XI (data for **1a** and **1b** are included for comparison). The temperature range over which kinetic data was obtained was not deemed adequate for an accurate separation of the free energy of activation into enthalpic and entropic contributions.⁴⁵

(43) Gutowsky, H. S.; Holm, C. H. *J. Chem. Phys.* **1956**, *25*, 1228.

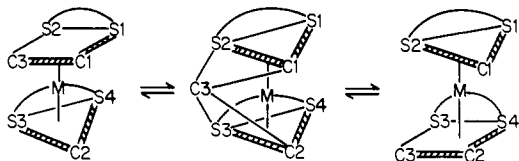
(44) (a) Anet, F. A. L.; Bourn, A. J. R. *J. Am. Chem. Soc.* **1967**, *89*, 760. (b) Faller, J. W. *Adv. Organomet. Chem.* **1977**, *16*, 211.

(45) Anet, F. A. L.; Ghiaci, M. *J. Am. Chem. Soc.* **1979**, *101*, 6857.

Scheme II



Scheme III



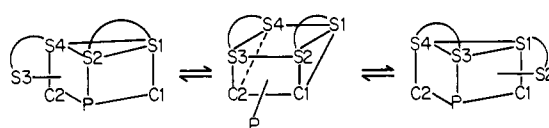
The narrow range of activation barriers, 8–10 kcal, exhibited by **2b**, **3b**, and **5b** is noteworthy, as is the observation that the high-energy exchange process of **1a** and **1b** also falls between these limits. In view of the structural correspondence between **1a** and **2b**, these ΔG^\ddagger values suggest that the single process evident in $W(CO)_2L(S_2CNR_2)_2$ complexes may be operative in the high-temperature $W(CO)_3(S_2CNR_2)_2$ exchange.

The ΔG^\ddagger values determined for $W(CO)_2L(S_2CNEt_2)_2$ complexes are somewhat dependent on the identity of the phosphorus donor ligand with the barrier decreasing in the order $PPh_3 > PEt_3 > P(OEt)_3$. This corresponds to decreasing steric requirements for the trivalent phosphorus ligand as reflected in the ligand cone angles (145, 132, and 109°, respectively).⁴⁶ The increased activation energy associated with larger ligands suggests that the rearrangement is intramolecular since larger ligands would be expected to decrease ΔG^\ddagger for a dissociative mechanism due to increased steric hindrance in the seven-coordinate ground state. Note that the order found is not compatible with electronic factors alone since the trialkylphosphine is the most basic of the three ligands investigated yet displays a barrier intermediate between the aryl and ethoxy phosphorus donors.

Confirmation that neither a carbonyl nor a phosphine ligand dissociates during the exchange process was provided by the retention of $^2J_{31P-W-13C}$ coupling information in the high-temperature limit. The observed two-bond coupling for **5b** (18 Hz) is the average of the two independent coupling constants measured at low temperature (see Table X).

Given the intramolecular character of the fluxionality exhibited by $W(CO)_2L(S_2CNR_2)_2$ complexes, one can consider plausible pathways which would equilibrate the two carbonyl environments on the NMR time scale. If one accepts the 4:3 geometry as an appropriate model for the static solution structure, a simple rearrangement scheme corresponding to movement of the phosphine ligand from the quadrilateral face into the trigonal face (Scheme II) is compatible with the experimental data. This motion would average the two carbon monoxide environments as well as the central carbons of the two dithiocarbamates. The oscillation from

Scheme IV



a 4:3 to a 3:4 geometry proposed as a possible mechanism for **2b** could also be extended to the high-energy fluxional process observed for **1** which averages the central dithiocarbamate carbon signals and all three of the carbonyl resonances¹¹ (Scheme III). This rearrangement coupled with the prior onset of the low-energy process that selectively exchanges C1 and C3 of **1** would effectively exchange all three of the CO sites as is observed. Note that the low-temperature process postulated to account for the fluxionality of **1** which averages only the C1 and C3 signals via rotation of the trigonal plane relative to the tetragonal base is not applicable to the two-carbonyl exchange of **2b** since the phosphine lies in the quadrilateral plane rather than in the trigonal face. In other words, if such a process were occurring in **2b**, it would interconvert two isomers with different coordination geometries and chemically and magnetically distinct phosphorus ligand positions. This contradicts the available data where only a single ^{31}P signal is observed over a wide range of temperatures.

A plausible alternative intramolecular rearrangement can be based on the more classical capped trigonal prism description if one selects S3 as the capping ligand above the S4–S2–C2–P quadrilateral face (CTP-2, Table VIII). Flexing the bidentate ligands to distort CTP-2 readily produces a new CTP of C_2 symmetry with P capping C1C2S2S3 such that C1–C2, S2–S3, and S1–S4 are pairwise equivalent due to the mirror plane which is present (Scheme IV). The ground-state isomer can then be formed with equal facility along either of two paths, to return to the S3 CTP-2 or to form the equivalent S2-capped trigonal prism. The phosphine environment is NMR equivalent in both permutational isomers while C1 and C2 have shifted between the capped quadrilateral face and the unique edge. Comparison of this rearrangement with the 4:3 process described above reveals a close correspondence in terms of the actual physical motion postulated for the two alternative idealized structures employed as ground-state models. The symmetrical species which must be traversed at some point along the reaction coordinate probably requires some movement of all the ligands, and the two rearrangements are in fact fundamentally similar to one another. The 4:3 description focuses on the triphenylphosphine motion while the capped trigonal prism mechanism concentrates on the details of the motion of the two chelate ligands.

Acknowledgment. This work was generously supported by a Cottrell Research Grant from Research Corp. and by the donors of the Petroleum Research Fund, administered by the American Chemical Society. The purchase of the diffractometer used in this research was made possible by NSF Grant CHE78-03064.

Supplementary Material Available: A listing of observed and calculated structure amplitudes (32 pages). Ordering information is given on any current masthead page.

(46) Tolman, C. A. *Chem. Rev.* 1977, 77, 313.